The quasi-cylindrical description of submerged laminar swirling jets

Antonio Revuelta[a)]
Departamento de Combustibles Fósiles, CIEMAT, 28040 Madrid, Spain

Antonio L. Sánchez
Area de Mecánica de Fluidos, Universidad Carlos III de Madrid, 28911 Leganés, Spain

Amable Liñán
E. T. S. I. Aeronáuticos, Pl. Cardenal Cisneros 3, 28040 Madrid, Spain

(Received 13 June 2003; accepted 11 December 2003; published online 4 February 2004)

The quasi-cylindrical approximation is used to describe numerically the structure of a submerged swirling jet for subcritical values of the swirl ratio $S \leqslant S_c$. The emerging flow structure is affected by the swirling motion, which enhances the entrainment rate of the jet and induces an adverse pressure gradient that reduces its momentum flux. The effect is more pronounced as the swirl ratio S is increased, yielding for sufficiently large values of S a jet with an annular structure. The integration describes the smooth transition towards the far-field self-similar solution for all values of S smaller than a critical value $S=S_c$, at which the numerical integration fails to converge at a given downstream location. The comparisons with previous experimental results confirm the correspondence between the onset of vortex breakdown and the failure of the quasi-cylindrical approximation. © *2004 American Institute of Physics.* [DOI: 10.1063/1.1645850]

This Brief Communication investigates the submerged swirling jet that forms when an incompressible fluid of density ρ and kinematic viscosity v discharges with both forward and swirling motion through a circular orifice of radius a into a stagnant region of the same fluid, a flow configuration recently studied experimentally by Billant *et al.*[1] The initial fluxes of momentum J and angular momentum L of the jet can be used to define the swirl ratio $S=L/(Ja)$ and the jet Reynolds number $R_j=[J/(\pi\rho)]^{1/2}/v$ as the main parameters characterizing the flow structure. The description below corresponds to moderately large values of R_j, for which the laminar jet remains steady, and to values of S of order unity, a distinguished regime that allows us to explore the effect of the swirl on the flow structure and the onset of vortex breakdown.[2–5]

Near the orifice, the jet is separated from the outer stagnant fluid by an annular mixing layer that thickens downstream, so that the effect of viscosity starts reducing significantly the velocity at the axis at distances of the order of R_j times the jet radius. The swirling motion causes the pressure near the axis to be smaller than the ambient value, which in turn induces an adverse axial pressure gradient that is largest at the axis.[3] For $S\sim O(1)$, the pressure differences induced are of the order of the dynamic pressure, so that the swirling motion results in a significant flow deceleration in the jet development region, additional to that associated with viscous stresses. The magnitude of the azimuthal flow velocity is seen to decay more rapidly that the axial velocity, so that in the far-field self-similar solution that arises at distances from the orifice much larger than $R_j a$ the pressure gradient induced no longer affects the forward motion at leading order.[6] For swirl ratios below a critical value of order unity, the jet remains slender, and can be therefore described with relative errors of order R_j^{-2} with the boundary-layer, or quasi-cylindrical (QC) approximation.[7] The resulting set of parabolic equations is integrated numerically by marching downstream from the orifice, providing a description for the jet development region independent of R_j. A smooth transition towards the far-field solution is observed only for swirl ratios below a critical value, $S=S_c$, for which the emergence of appreciable axial gradients precludes the convergence of the numerical scheme at a given downstream location. According to Hall,[3] this failure of the QC approximation corresponds to the onset of vortex breakdown, a point supported by the experimental observations,[1] which indicate that the critical conditions for vortex breakdown are practically independent of R_j. It should be noted that, although the critical swirl number can be predicted with the boundary-layer approximation, the description of the emerging vortex requires consideration of the full Navier–Stokes equations, as done in Ref. 8 for the submerged jet.

To write the conservation equations for continuity and momentum in the QC approximation it is convenient to introduce as scales for the different variables those corresponding to the development region. Thus, the radial and axial coordinates measured from the orifice center r and x are scaled with the radius a and with the characteristic length $R_j a$, respectively, while the characteristic radial and axial velocities v/a and $u_c=[J/(\pi\rho)]^{1/2}/a$ are used to define the dimensionless velocity components v and u and the pressure difference from the ambient value is nondimensionalized with its characteristic value ρu_c^2 to give the variable p. The swirling motion is measured by the circulation of the azimuthal velocity, which is scaled with its characteristic value

a)Electronic mail: a.revuelta@ciemat.es

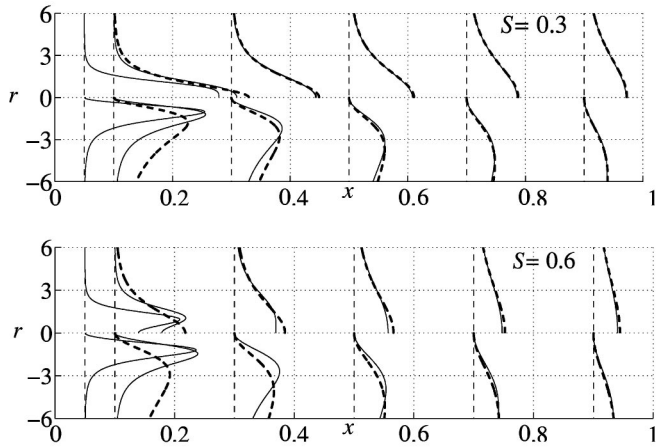

FIG. 1. Profiles of velocity (upper half) and circulation (lower half) corresponding to $S=(0.3,0.6)$ obtained from numerical integration of the QC equations (solid lines) and from evaluations of the far-field asymptotic expressions (dashed lines).

$L/(\rho u_c a^2/2)$ to give the dimensionless variable Γ. The problem reduces to that of integrating

$$\frac{\partial u}{\partial x}+\frac{1}{r}\frac{\partial (rv)}{\partial r}=0, \tag{1}$$

$$u\frac{\partial u}{\partial x}+v\frac{\partial u}{\partial r}+\frac{\partial p}{\partial x}=\frac{1}{r}\frac{\partial}{\partial r}\left(r\frac{\partial u}{\partial r}\right), \tag{2}$$

$$\frac{\partial p}{\partial r}=S^2\frac{\Gamma^2}{r^3}, \tag{3}$$

$$u\frac{\partial \Gamma}{\partial x}+v\frac{\partial \Gamma}{\partial r}=r\frac{\partial}{\partial r}\left(\frac{1}{r}\frac{\partial \Gamma}{\partial r}\right), \tag{4}$$

for $x>0$ with the boundary conditions $\partial u/\partial r=v=\Gamma=0$ at $r=0$ and $u=\Gamma=p=0$ as $r\to\infty$, and with the initial conditions at $x=0$ given by $u=u_i(r)$ and $\Gamma=\Gamma_i(r)$ for $0\leqslant r\leqslant 1$ and $u=\Gamma=0$ for $r>1$. Here, $S=L/(Ja)$ is the swirl ratio and $u_i(r)$ and $\Gamma_i(r)$ are, respectively, the distributions of axial velocity and circulation at the jet exit. The integrations shown in Figs. 1–3 correspond in particular to a jet with

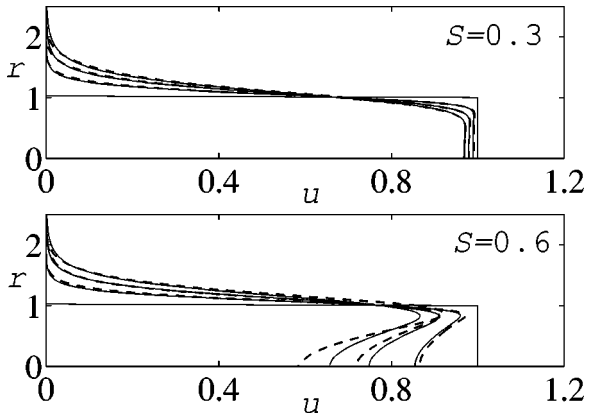

FIG. 2. Axial velocity profiles for $S=(0.3,0.6)$ and different axial positions $x=(0.0,0.005,0.01,0.015)$ obtained from numerical integration of the QC equations (solid lines) and from evaluations of the asymptotic profile at $x\ll 1$ (dashed lines).

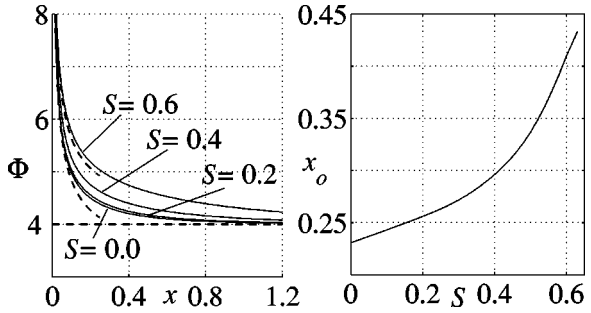

FIG. 3. The function $\Phi(X)$ and the virtual origin x_o for different values of the swirl number S; dashed lines represent the asymptotic values for $x\ll 1$ ($S=0.0$ and $S=0.6$) and $x\gg 1$.

uniform axial velocity $u_i=1$ and with solid body rotation $\Gamma_i=2r^2$.

As can be shown by radial integration of combinations of (1) and (4) and of (1) and (2), the solution to the above problem satisfies the conservation of angular momentum flux $\int_0^\infty 2ru\Gamma\,dr=1$ along with the momentum balance equation $M=\int_0^\infty 2r(u^2+p)dr$, where the constant M is the so-called flow force.[6] The latter equation describes how the momentum flux, $\int_0^\infty 2ru^2dr$, which with the scaling selected here takes the value $\int_0^1 2ru_i^2dr=1$ at $x=0$, decreases due to the adverse pressure gradient as the jet develops. In the far-field region corresponding to $x\gg 1$ the pressure differences from the ambient value, given below in (7), can be neglected in the momentum balance, so that in this region the rescaled momentum flux becomes $\int_0^\infty 2ru^2dr=M$. The value of $M=1+\int_0^1 2rp_i dr<1$ depends on the negative radial pressure distribution at the jet exit, $p_i(r)=-S^2\int_r^1(\Gamma_i^2/r^3)dr$, a function of the initial circulation $\Gamma_i(r)$ to be computed from (3), yielding for instance $p_i=-2S^2(1-r^2)$ and $M=1-S^2$ for initial solid-body rotation $\Gamma_i=2r^2$. Note that the condition $M>0$ imposes the limitation

$$S<\left\{\int_0^1 2r\left[\int_r^1(\Gamma_i^2/r'^3)dr'\right]dr\right\}^{-1/2}, \tag{5}$$

to the swirl level that enables the establishment of a slender jet.

The computation of the jet development region corresponding to $x\sim O(1)$ requires the numerical integration of (1)–(4). For $x\ll 1$ the mixing layer that develops from the orifice rim admits a self-similar description, which depends on the values of u_i and Γ_i near $r=1$. The leading-order solution for the axial and radial velocity is independent of the swirl and, for $u_i=1$, corresponds to the Chapman–Lessen planar mixing layer,[9,10] which can be described by introducing the stream function $\Psi=x^{1/2}(F_0(\xi)+x^{1/2}F_1(\xi)+\cdots)$, together with the scaled variable $\xi=(r^2-1)/(2x^{1/2})$, which is written following[6] in a form that facilitates the description of annular mixing layers. If the prime $'$ denotes differentiation with respect to ξ, then the leading-order problem reduces to that of integrating $F_0'''+F_0F_0''/2=0$ with boundary conditions $F_0'(-\infty)-1=F_0'(\infty)=0$, as corresponds to matching with the outer velocity profile, and $F_0(-\infty)-\xi=0$, as corresponds to the condition that, at this order, the mixing layer entrains fluid only from the outer stagnant side. One can

easily verify that, for solid body rotation [$\Gamma_i(r\to 1)=2$], the leading-order terms in the accompanying expansions for the circulation $\Gamma=2[G_0(\xi)+x^{1/2}G_1(\xi)+\cdots]$ and pressure $p=x^{1/2}[P_0(\xi)+x^{1/2}P_1(\xi)+\cdots]$ reduce to $G_0=F_0'$ and $P_0=4S^2(F_0'F_0+2F_0'')$.

In the jet core, corresponding to radial distances $1\geqslant 1-r\gg x^{1/2}$, the initially uniform velocity profile presents for $x\ll 1$ small perturbations of order x. The perturbed solution in this inviscid region can be expressed in the form $1-u=p+2S^2(1-r^2)=4xv_1SJ_0(4Sr)/J_1(4S)$ and $rv=(2r^2-\Gamma)/(4x)=v_1rJ_1(4Sr)/J_1(4S)$, with J_0 and J_1 representing Bessel functions of the first kind. The unknown value v_1 of the radial velocity as $r\to 1$ can be determined from the analysis of the first-order corrections in the mixing layer, where the radial velocity and the pressure must match with the $O(x)$ perturbations in the jet. Thus, integrating $F_1'''+F_0F_1''/2-F_0'F_1'/2+F_0''F_1-(P_0-\xi P_0')/2+2F_0''+2\xi F_0'''=0$, $G_1''+F_0G_1'/2-F_0'G_1/2+F_1G_0'+2\xi G_0''=0$ and $P_1'-8S^2G_0G_1+4\xi P_0'=0$ with boundary conditions $F_1'(-\infty)=F_1'(\infty)=F_1(-\infty)+v_1=G_1'(\infty)=G_1'(-\infty)-2\xi=P_1(\infty)=P_1(-\infty)-4Sv_1J_0(4S)/J_1(4S)=0$ provides for a given value of S the first-order corrections F_1, G_1, and P_1 along with the value of v_1, giving for instance $v_1=(0.9790,6.6542)$ for $S=(0.3,0.6)$.

Note that the asymptotic analysis for $x\ll 1$ should be modified when the initial profiles differ from those considered here. In particular, concerning the validity of the results obtained for $u_i=1$ and $\Gamma_i=2r^2$, the boundary-layer that develops on the duct wall upstream from the orifice necessarily modifies the character of the mixing layer in the vicinity of the jet exit, so that the description given above only holds for axial distances in the range $\varepsilon^2\ll x\ll 1$, where εa is the characteristic value of the boundary-layer thickness.

A self-similar solution also exists at $x\gg 1$,

$$\frac{3u}{512M}=\frac{\Gamma}{16\eta^2}=\frac{1}{x+x_o}\frac{1}{(64/3+\eta^2)^2}, \tag{6}$$

in which the axial velocity corresponds to Schlichting solution[11] for the swirl-free jet, while the solution for the circulation and the accompanying pressure difference from the ambient

$$p=-\frac{MS^2}{(x+x_o)^4}\frac{128/3}{(64/3+\eta^2)^3}, \tag{7}$$

are due to Görtler[12] and Loitsianskii.[13] In the above description, $\eta=M^{1/2}r/(x+x_o)$ is the similarity coordinate and x_o is the so-called virtual origin, which is equal for the velocity and circulation profiles. As explained in Ref. 14, this virtual origin arises as the first-order correction in the far-field asymptotic description for large distances. Its computation requires consideration of the jet development region for $x\sim O(1)$, giving a value that depends on S and on the shape functions $u_i(r)$ and $\Gamma_i(r)$. Note that the Schlichting–Görtler–Loitsianskii asymptotic solution is fundamentally different from the asymptotic solutions given by Long[15] and Fernández-Feria *et al.*[16] for jets with outer circulation, in that the axial and azimuthal motions remain intimately coupled in the latter solutions.

Results of integrations of (1)–(4) for $x\sim O(1)$ are shown in Figs. 1–3. A three-level implicit method with second-order approximation schemes for spatial derivatives was used to integrate the parabolic QC equations, with an iterative process to adjust the values of p, Γ, and v at every axial position. Typical values of the grid spacing are $\delta r=10^{-2}$ and $\delta x=10^{-3}$, with finer grids being needed for increasing S. Profiles of u and Γ at different downstream locations and for two different values of $S<S_c$ are plotted in Fig. 1, where the dashed lines indicate the corresponding far-field solutions given in (6). The evolution of the velocity profiles at small distances from the orifice is displayed in Fig. 2, where the numerical results are compared with the asymptotic solution obtained by adding the core velocity deficit $-4xv_1SJ_0(4Sr)/J_1(4S)$ evaluated for $r\leqslant 1$ to the two-term mixing-layer expansion $F_0'+x^{1/2}F_1'$. Figure 3 shows the entrainment rate $\Phi(x)=-(rv)_{r\to\infty}$ for different values of S, a decreasing function that evolves from the asymptotic value $\Phi=[x^{-1/2}(F_0-\xi F_0')/2+F_1-\xi F_1'/2]_{\xi\to\infty}$, corresponding to $x\ll 1$, to the constant value $\Phi=4$ corresponding to Schlichting solution[11] for $x\gg 1$. As can be seen, the presence of swirl modifies significantly the rate at which the outer fluid is entrained by the jet in the jet development region $x\sim O(1)$, which changes the jet volume flux

$$\int_0^\infty 2ru\,\mathrm{d}r=q+2\int_0^x\Phi(x)\,\mathrm{d}x, \tag{8}$$

where $q=\int_0^1 2ru_i\,\mathrm{d}r$ is the initial jet volume flux at the orifice scaled with its characteristic value πa^2u_c. Evaluating (8) at $x\gg 1$ reveals that the virtual origin x_o amounts to a correction of order unity in the far-field volume flux, with the value of $x_o=q/8+\int_0^\infty(\Phi/4-1)\,\mathrm{d}x$ accounting for the initial volume flux and also for the increased entrainment rate taking place in the jet development region.[14] The dependence of x_o on S is given in Fig. 3 for $u_i=1$ and $\Gamma_i=2r^2$.

The adverse pressure gradient induced by the swirl leads to the formation of an annular jet for sufficiently large values of S ($S\gtrsim 0.5$ for $u_i=1$ and $\Gamma_i=2r^2$), with an off-axis velocity maximum initially located on the inner side of the mixing layer that develops from the orifice. This annular jet can be clearly observed in the results of Figs. 1 and 2 for $S=0.6$. For this swirl level the annular jet is seen to evolve to eventually approach the self-similar far-field solution given in (6). A smooth transition could not be achieved as the value of S was increased to the critical value $S=S_c=0.64$, connected with vortex breakdown,[3] at which no convergence of the numerical scheme could be obtained at $x\simeq 0.025$. As in the calculations reported in Ref. 17, the failure is associated with large values of the radial velocity v accompanying a rapid deceleration of the flow along the axis.

The value of S_c, to be determined numerically, depends on the initial profiles u_i and Γ_i. Clearly, the limitation $M>0$ provides an upper boundary for the value of S_c, which must therefore satisfy (5). As explained in Ref. 1, a lower boundary for S_c follows from the condition that vortex breakdown is associated with the appearance of a stagnation point along the axis. If the flow is assumed to be arrested

inviscidly, then conservation of total head along the axis provides the expression

$$S_c > \left[(u_i(0)^2/2) \Big/ \int_0^1 (\Gamma_i^2/r^3)\mathrm{d}r \right]^{1/2} \tag{9}$$

involving the initial velocity at the axis $u_i(0)$ and the initial distribution of circulation. The expressions (5) and (9) provide upper and lower bounds for S_c. For instance, for the initial conditions considered, the critical swirl ratio must be in the range $1/2 < S_c < 1$, in agreement with the result $S_c = 0.64$ obtained.

Finally, we shall investigate the accuracy with which the failure of the boundary-layer approximation can be used as a criterion to determine the swirl ratio at breakdown in the case of submerged jets. For this purpose, integration of (1)–(4) was started using as initial profiles $u_i(r)$ and Γ_i those measured experimentally near the injector mouth by Billant *et al.*[1] In their analysis, the swirl ratio S^* was defined as twice the ratio of the maximum azimuthal velocity to the maximum axial velocity at the jet exit, so that

$$S^*/S = 2(\Gamma_i/r)_{\max}/(u_i)_{\max}. \tag{10}$$

The profiles used in the numerical integration correspond to the near-critical conditions given in Figs. 4 and 24 of Ref. 1 for $S^* = 1.33$, which were scaled according to the formulation used here. Integrations were performed for increasing values of S. An annular jet was seen to form for $S \gtrsim 0.39$ and failure to converge occured for $S_c = 0.50$. The critical value at breakdown in the experiments[1] was $S_c^* = 1.3-1.4$, with only small variations in the range of Reynolds numbers investigated and for the two different injectors used. According to (10), this experimental value corresponds in our formulation to a critical value $S_c = 0.45-0.48$, in close agreement with the value $S_c = 0.50$ computed in the QC approximation.

ACKNOWLEDGMENTS

This collaborative research was supported by the Spanish MCyT under Project# DPI2002-04550-C07. A.R. acknowledges also the financial support of the MCyT through the Ramon y Cajal Program.

[1] P. Billant, J. M. Chomaz, and P. Huerre, "Experimental study of vortex breakdown in swirling jets," J. Fluid Mech. **376**, 183 (1998).
[2] M. P. Escudier, "Vortex breakdown: Observations and explanations," Prog. Aerosp. Sci. **25**, 189 (1988).
[3] M. G. Hall, "Vortex breakdown," Annu. Rev. Fluid Mech. **4**, 195 (1972).
[4] S. Leibovich, "The structure of vortex breakdown," Annu. Rev. Fluid Mech. **10**, 221 (1978).
[5] V. Shtern and F. Hussain, "Collapse, symmetry breaking, and hysteresis in swirling flows," Annu. Rev. Fluid Mech. **31**, 537 (1999).
[6] L. Rosenhead, *Laminar Boundary Layers* (Dover, New York, 1963).
[7] M. G. Hall, "The structure of concentrated vortex cores," *Progress in Aeronautical Sciences, Vol. 7* (Pergamon, New York, 1966), pp. 53–110.
[8] W. Kollmann, A. S. H. Ooi, M. S. Chong, and J. Soria, "Numerical simulation of vortex breakdown in swirling jets," Comput. Fluid Dynamics **376**, 63 (2001).
[9] D. R. Chapman "Laminar mixing of a compressible fluid," NACA-TN-1800 (1949).
[10] M. Lessen, "On the stability of the laminar free boundary between parallel streams," NACA-R-979 (1950).
[11] H. Schlichting, "Laminare strahlausbreitung," Z. Angew. Math. Mech. **13**, 260 (1933).
[12] H. Görtler, "Decay of swirl in an axially symmetrical jet, far from the orifice," Revista Matematica Hispanoamericana **14**, 143 (1954).
[13] L. G. Loitsianskii, "Propagation of a whirling jet in an infinite space filled with the same fluid," Prikl. Mat. Mekh. **17**, 3 (1953), in Russian.
[14] A. Revuelta, A. L. Sánchez, and A. Liñán, "The virtual origin as a first-order correction for the far-field description of laminar jets," Phys. Fluids **14**, 1821 (2002).
[15] M. G. Long, "A vortex in an infinite viscous fluid," J. Fluid Mech. **11**, 611 (1961).
[16] R. Fernández-Feria, J. Fernández de la Mora, and A. Barrero, "Solution breakdown in a family of self-similar nearly inviscid axisymmetric vortices," J. Fluid Mech. **305**, 77 (1995).
[17] M. Pérez-Saborid, M. A. Herrada, A. Gómez-Barea, and A. Barrero, "Downstream evolution of unconfined vortices: Mechanical and thermal aspects," J. Fluid Mech. **471**, 51 (2002).